

Received 13 August 2022, accepted 5 September 2022, date of publication 19 September 2022,
date of current version 30 September 2022.

Digital Object Identifier 10.1109/ACCESS.2022.3207925

TOPICAL REVIEW

Adaptive Unscented Kalman Filter for Robot Navigation Problem (Adaptive Unscented Kalman Filter Using Incorporating Intuitionistic Fuzzy Logic for Concurrent Localization and Mapping)

YONG FANG¹, AMIR PANAH², JAVAD MASOUDI³, BEHNAMEH BARZEGAR^{1,2}, AND SAEED FATEHI⁴

¹Department of Traffic and Transportation, Chongqing Jiaotong University, Chongqing 400000, China

²Department of Computer Engineering, Babol Branch, Islamic Azad University, Babol 47471-37381, Iran

³Department of Computer Engineering, Sari Branch, Islamic Azad University, Sari 48161-19318, Iran

⁴Department of Computer Engineering, University College of Allameh Helli Chalus, Chalus 4661966854, Iran

Corresponding author: Behnam Barzegar (barzegar.behnam@yahoo.com)


ABSTRACT The navigation of a mobile robot is a very important issue, especially for an autonomous mobile robot. A robot autonomously can track the area by interpreting the arena, building an adequate map, and localizing itself to this map. This paper proposes a Hybrid filter for Concurrent Localization and Mapping (CLAM) in the navigation to rectify the faults, basically Unscented Fast Simultaneous Localization and Mapping (SLAM) (UFS). We also interrogate the effectiveness of the IF system to investigate nonlinear attributes. A probabilistic method has planned the solution to the CLAM issue, which is an essential requirement for the navigation of robots. The Hybrid filter CLAM contains an Intuitionistic Fuzzy Logic (IFL) and Unscented Kalman Filter (UKF). The IFL is first ordered by using a correctness function explained on score functions for the non-membership function (NMF) and membership function (MF) of the IFL. Then this ordering is utilized to develop a method for a sufficient decision on the CLAM issue. The proposed method has a few privileges in management robot navigation with nonlinear movements owing to the inference feature of the IFL, which also needs a fewer quantity of comparisons than the UFS and shows much better efficiency from the robustness, perspective assessment exactitude, and reliability than the UFS, also, for learning the measurement and control noise covariance matrices for increasing correctness and consistency are utilized IFL. The Hybrid filter CLAM proficiency compared with the UFS has a smaller quantity of computations and good efficiency for bigger areas as demonstrate in the results of simulation and experimental.

INDEX TERMS Intuitionistic fuzzy logic, unscented Kalman filter, navigation, hybrid filter, CLAM.

I. INTRODUCTION

Navigation is one of the most main problems for a mobile robot as the mobile robot keeps follow of its location via retaining a map of environments and an estimate of its location on that map. The investigation attempts on mobile robots have mainly paid attention on problems. One of the significant issues for robots as the robots keeps track of their posi-

tion by holding an outline of areas and an assessment of their localization is navigation. In addition, data from a Frequency-Modulated Continuous-Wave (FMCW) Radar, Inertial Measurement Unit (IMU) and encoders that are capable of withstanding fire environments were fused to localize the robot in indoor fire environments [1]. The SLAM is the most generic widely investigated main subfields of mobile robots. For solving the SLAM issues, statistical methods, such as Bayesian filters, have attained extensive acknowledgment. Certain of the more general methods consist of the Kalman

The associate editor coordinating the review of this manuscript and approving it for publication was Yu-Da Lin .

36 filter family and particle filter (PF). To achieve consensus
37 estimation, each sensor node is allowed to communicate with
38 its neighboring nodes according to a prescribed communica-
39 tion topology. Firstly, a new hybrid consensus-based filtering
40 algorithm under random link failures, which affect the infor-
41 mation exchange between sensors and are modeled by a set of
42 independent Bernoulli processes, is designed via redefining
43 the interaction weights. Second, a novel observability condi-
44 tion, called parameterized jointly uniform observability is
45 proposed to ensure the stochastic boundedness of the error
46 covariances of the hybrid consensus-based filtering algorithm
47 [2]. A robust UKF under a quaternion-error method is pro-
48 posed for the assessment in the presentment of measurement
49 flaws. This method utilizes a statistic function containing
50 measurement residuals to discover measurement flaws and
51 then utilizes a conformity plan under the multiple measure-
52 ment criterion items for filter efficiency versus defective
53 measurements. The robust UKF, the EKF, and UKF are also
54 implemented under the same simulation conditions, to com-
55 pare the estimated efficiency of the proposed method [3].
56 The FastSLAM (FS) has two main restrictions, that involve
57 the Jacobian computations and the nonlinear functions linear
58 estimates. These can create inconsistencies. Another vital
59 issue is to decline the number of probes whenever keeping
60 the assessment exactitude. The proposed method under the
61 scaled unscented transformation (UT) is called the UFS.
62 It dominates the significant drawbacks of the past research
63 via straightly using nonlinear relations. The results in harsh
64 environments are offered, representing the superiority of the
65 UFS [4]. Using robust model prediction offered a novel
66 UKF. This strategy compounds framework driving noise in
67 framework state via increase of state span size to extend the
68 input of systems state data. The framework model blame
69 is made through show forecast and is utilized to refine the
70 unscented Kalman filter (UKF) procedure to attain the assess-
71 ment of the genuine framework state. The proposed method
72 creates the strength of the UKF, therefore overbearing the
73 constraint that the UKF is influenced via a framework model
74 error. The experimental results illustrate that the convergence
75 rate and precision of the proposed method are premieres
76 to the UKF and EKF [5]. A robust controller proposed for
77 actuators helicopter control in attendance of actuator and
78 sensor errors. The proposed method allows evading effort-
79 ful modeling, declining the number of rules for the fuzzy
80 overseer, attenuating the chattering efficacy of the sliding
81 manner control, and assuring the consistency of the system.
82 This method can greatly diminish the chattering performance,
83 exploring good in the attendance of actuator and sensor
84 errors. This method allows evading effortful modeling, reduc-
85 ing the number of rules for the fuzzy controller, attenuating
86 the chattering efficacy of the sliding manner control, and
87 assuring the consistency of the system. The results show
88 that this method can greatly diminish the chattering perfor-
89 mance, exploring good in the attendance of actuator and
90 sensor errors [6]. Two fuzzy preprocessing approaches were
91 presented, utilizing an intuitionistic fuzzy set and the fuzzy

set to standard datasets. Using three existent gene expression 92
datasets, the fuzzy normalization methods were compared 93
with two standard normalizations also a raw gene phrase. The 94
exactitude of selected features was distinguished using The 95
classifiers of random forest, k-nearest-neighbor, and support 96
vector machine. The results demonstrate that the intuitionistic 97
fuzzy set is better than the fuzzy set normalization [7]. They 98
propose for path tracking and autonomous navigation the 99
utilizing of the calculated roughly state vector in a control 100
chain. The rough calculation of the robot position vector is 101
accomplished with the utilization of PF, Sigma-Point Kalman 102
Filtering (SPKF), extended Kalman filter (EKF), and a new 103
nonlinear roughly calculation approach that is the Derivative- 104
free nonlinear Kalman Filtering (DKF). Comparing these 105
filtering methods to roughly calculation exactitude and speed 106
of computation, DKF demonstrates that the SPKF is a trust- 107
worthy and computationally effective method to control state 108
roughly calculation. Also, the DKF is speedier than the other 109
filters when so successful in exact, to variance, state roughly 110
calculations [8]. 111

The neural network is learned using heuristic optimization 112
to train the remaining error of the motion model, which is 113
then augmented to the odometry data to attain the fulfill- 114
ment motion model estimate. heuristic optimization is uti- 115
lized, to match any kind of cost function. The prediction and 116
correction are applied concurrently within our new method, 117
which merges the motion and sensor models. A heuristic 118
method is applied to progressively rectify the neural model 119
till it generates a path that is most solid with the real sensor 120
measurements. The novel method does not need any previous 121
wisdom of the motion or sensor models and offers the sensor 122
noise and good efficiency irrespective of the mobile robot, 123
during this training procedure always. Moreover, it does not 124
need the data association stage at loop closing which is vital 125
in many other SLAM methods but can still create a correct 126
map. The results in different harsh areas with a kind of noise 127
display which the training ability of novel methods certifies 128
efficiency which is always less sensitive to noise and more 129
correct than that of other SLAM methods [9]. Adaptive Neu- 130
ral Network Unscented Kalman Filter (ANFUKF) has been 131
applied to the attribute position's assessment and PSO (Parti- 132
cle Swarm Optimization) has been applied to the mobile robot 133
pose assessment. The results demonstrate that approximated 134
exactitude and the consistency of the proposed method are 135
excellent for FS. Also, in this method to attain better consis- 136
tency, the adaptive Neuro-fuzzy incorporates square root cen- 137
tral distinction Kalman Filter (KF) utilized for the attribute 138
position's assessment. In addition, will decrease the number 139
of particles and the computational complexity [10]. A novel 140
method proposed with a fuzzy 3D grid explained by dual 2D 141
grid maps for self-navigation. A syntactic preprocessing is 142
proposed to carry out positioning via substitution amongst 143
the weighted three and two-point positioning approach and 144
the weighted average localization approach. The presented 145
approach has better attributes in the robustness of navigation 146
and fewer calculations than the other methods. Fuzzy logic is 147

used to optimize the parameters of a Fuzzy Logic Controller (FLC's) function to find the best rational controller for an automated robot. Because discontinuous endpoint friction is undetectable to the pressure of the fluid internally, feedback from traditional external force using force/tactile sensing is preferred. As a result, a fuzzy-based control using linear feedback was developed and used to test the integrated system's response dynamically and location accuracy [11]. The UKF utilizes the UT (Unscented Transformation) but the EKF that applies different types of nonlinear functions. Non-differentiable MFs can be Intended on the Takagi-Sugeno (TS) models. This makes to be appropriate for the online item computing of vast classes of TS. The results determine the advantage of proposed methods and efficiency betterment according to the root mean square of the assessment error [12]. An efficiency of fuzzy logic controllers is proposed by the heuristic learning method. The robots should be able to train with dynamic changes in their surroundings. An appropriate tool for the navigation of robots is the Fuzzy logic control. The ameliorated efficiency of fuzzy logic is controlled by evolutionary training methods. This method deals with automatically training to adjust the MF parameters for robot motion control [13]. Tracking of area mobile objects is significant for the expansion of robot navigation. The presented fuzzy controller according to numerous input systems to adjust noise covariance the advancement arrangement of a KF. This proposed method has a good efficiency for the object tracking issue on standard KF because of its ability to recover the filter divergence issue [14]. Incertitude measures can carry out a new opinion for analyzing wisdom transmitted. Also, incertitude measurement is a key subject, similar to the role in probability theory. The existing measures of incertitude cannot attain all schemas of incertitude. An incertitude measure including these three uncertainties is proposed, generally. In addition, the presented incertitude measure can discriminate incertitude concealing in classical sets. It supplies an alternative approach to creating unified incertitude measures [15]. They propose a new method that utilizes the sterling interpolation approach using the Cholesky decomposition approach confronted with the nonlinear system issue. This method not only declines the local linearization truncation error but also warrants the positive definitive feature of the covariance matrix. It updates any sigma point (SP) utilizing a novel method that attains optimum filter gain via the Strong Tracking Filter online tuning factor and excludes indecisive noise. The proposed method is much better efficiency in assessment correctness, talent, and capability than Central Difference FS [16]. An amended significance sampling is presented under the transformed UKF to amend the efficiency of the FS. The amendment is combined with a novel fuzzy noise estimator, that can regulate the state noises online and observation under the related residual, covariance and so decline the faults caused by model inexactitude, generally. An adaptive resampling is presented to substitute the conventional resampling to prevail over these defects, retrieved from genetic optimization [17]. Normalized

cross-correlation is unpopular for its high computing cost; anyway, it is plump for illumination situations between two cameras. It is practical in real-time stereo systems, rarely. The computational complexity has no relationship with the matching window size. The novel method has fewer computing costs [18]. A Genetic approach is carried out to construct a collision-free optimum path joining an initial configuration. This approach is operated to smooth the optimal route built via transition, the sufficient left and right velocities to continue exploring on the desired smoothed route are designated. Kinect sensors and odometry sensors are operated to estimate the position of the robot and current orientation using KF [19]. Decision-makers can eliminate the reception degree, the refusal degree, the reception degree, and the hesitation degree, with the help of the Intuitionistic Fuzzy theory. These are unknown quantities with incertitude. So, to Cope with the incertitude with suspicion the Intuitionistic Fuzzy theory seems to be more trusty than the Fuzzy Set theory. This nominates several concepts, including the fuzzy theory and the Intuitionistic Fuzzy. In this paper, we propose a Hybrid filter CLAM for depreciatory incertitude in comparison to the UFS. We also interrogate the effectiveness of the IF system to investigate nonlinear attributes. A review of the UKF method is explained in part 2, and the Hybrid filter CLAM is proposed in part 3. Part 4 demonstrates the simulation and experimental results of the UFS and Hybrid filter CLAM. Part 5 discussed Concluding.

II. REVIEW OF THE UKF METHOD

The UT under the transformation in the UKF is expanded [20]. In the UKF isn't a need to calculate the Jacobian matrix [21]. The UKF is choosing a special quantity of points from the previous landmarks [22]. The state model of robot motion is given as per the following:

$$\begin{cases} x_k = f(x_{k-1}, u_{k-1}) + w \\ z_k = Hx_k + V_k \end{cases} \quad (1)$$

wherein z_k and u_{k-1} are the output and input vectors and x_k is the state vector, k index is the time stage. The covariance matrix of procedure noise (CMPN) is displayed with Q_k and the CMPN vector is displayed with w_k . H is the observation matrix. The covariance matrix of measurement noise (MNCM) is displayed with R_k and MNCM vectors are displayed with V_k .

Given the error covariance matrix P_{k-1} , the state vector \hat{x}_{k-1} and the Sigma Points (SPs) $X_{i,k-1}$ are as per the following:

$$\begin{cases} X_{i,k-1} = \hat{x}_{k-1} & i = 0 \\ X_{i,k-1} = \hat{x}_{k-1} + (a\sqrt{nP_{k-1}}) & i = 1, \dots, n \\ X_{i,k-1} = \hat{x}_{k-1} - (a\sqrt{nP_{k-1}}) & i = L + 1, \dots, 2n \end{cases} \quad (2)$$

The scalar a is a little positive amount and decides the expansion of the SPs around \hat{x}_{k-1} . The i th column of the square root of the matrix P is displayed with $(\sqrt{P})_i$.

252 The novel SPs are operating via the UT and transition
253 function f on the past SPs:

$$254 \quad X_{i,k} = f(X_{i,k-1}, u_{k-1}) \quad (3)$$

255 The predicted mean as per the following:

$$256 \quad \hat{x}_k = \sum_{i=0}^{2n} w_i X_{i,k} \quad (4)$$

257 And the covariance of error as per the following:

$$258 \quad P_k = \sum_{i=0}^{2n} w_i (X_{i,k} - \hat{x}_k) (X_{i,k} - \hat{x}_k)^T + Q_k \quad (5)$$

259 wherein \hat{x}_k is the predicted amount of a state parameter, P_k is
260 the mean squared error of \hat{x}_k , w_i is the SPs weight and $X_{i,k}$ is
261 the updated sampling point, a is a constant, illustrated as per
262 the following:

$$263 \quad \begin{cases} w_i = 1 - \frac{1}{a^2} & i = 0 \\ w_i = \frac{1}{2na^2} & i = 1, \dots, 2n \end{cases} \quad (6)$$

264 The SPs measurements are formulated as per the following:

$$265 \quad Z_k = H(X_{i,k} - u_k) \quad (7)$$

266 The predicted measurements weighted mean as per the
267 following:

$$268 \quad \bar{Z}_k = \sum_{i=0}^{2n} w_i Z_k \quad (8)$$

269 The UKF updated measurement as per the following:

$$270 \quad P_{x_k x_k} = \sum_{i=0}^{2n} w_i (Z_k - \bar{Z}_k) (Z_k - \bar{Z}_k)^T + R_k \quad (9)$$

$$271 \quad P_{x_k y_k} = \sum_{i=0}^{2n} w_i (X_{i,k} - \hat{x}_k) (Z_k - \bar{Z}_k)^T \quad (10)$$

$$272 \quad K_k = P_{x_k y_k} P_{x_k x_k}^{-1} \quad (11)$$

$$273 \quad \hat{x}_k = \hat{x}_k + K_k (Z_k - \bar{Z}_k) \quad (12)$$

$$274 \quad P_k = P_k - K_k P_{x_k x_k} K_k^T \quad (13)$$

275 wherein $P_{x_k x_k}$ is the predicted measurement covariance
276 parameter, $P_{x_k y_k}$ is the covariance parameter between the
277 measurement and state, K_k is the Kalman gain, P_k is the
278 covariance parameter and \hat{x}_k is the state assessment [23].
279 Stages 1–3 were repeated until all parameters were computed.

280 III. CLAM ALGORITHM USING THE HYBRID FILTER

281 As the core of the proposed method is the betterment of errors
282 towards UFS processing via the learning procedure, the IFL
283 is very important. The IFL can carry out as a fast and precise
284 tool approximating via observed data. In the UFS, the mea-
285 surement data is very effective for the learning procedure that
286 can be obtained via several types of sensors. Inference proce-
287 dures, calculating the weight, are effective to ameliorate the
288 exactitude via decreasing the robot pose's errors. The IFL is
289 very effective in declining the time of computation and incre-
290 menting the exactitude of CMPN and MNCM, especially.
291 Also, it increments the exactitude of choosing SPs when mov-
292 ing the robot upon various routes from various observation

things, and this will increment the robot movement reliability. 293
the proposed method requires learning about fundamental 294
information via observation stages of the proposed method. 295
Also, the computation time declined. Significant inputs are 296
the covariance and mean that is computed via previous input, 297
 u_{k-1} and exposure input, u_k . The robot computes the previous 298
covariance and means in a prediction stage, in an observation 299
stage, it computes a Kalman gain, suggesting covariance and 300
mean described attributes [24]. Using the learning procedure, 301
the IFL as the core of the proposed method is the complemen- 302
tation of errors in the UFS procedure. The IFL can be used as 303
a quick and exact means of approximating a mapping under 304
data seen. 305

306 A. THE BEST SPs CHOOSING IN THE HYBRID FILTER 307 CLAM

308 For solving a CLAM issue having incertitude and hesitation
309 in the prediction of the robot position, one describes a CLAM
310 as having intuitionistic fuzzy localization exactitude. The
311 CMPN or MNCM of probabilities model, that are related to
312 the IFL, as per the following:

$$313 \quad O_{ij} = \begin{bmatrix} O_{11} & O_{12} & \dots & O_{1j} \\ O_{21} & O_{22} & \dots & O_{2j} \\ \vdots & \vdots & \dots & \vdots \\ O_{i1} & O_{i2} & \dots & O_{ij} \end{bmatrix} = RorQ \quad (14)$$

314 wherever $i, j = 1, 2, \dots, r$, and r is the quantity of SPs. Com-
315 puting the matching probabilities of SPs in diverse observa-
316 tions with possibility matrix O_{ij} and the Gaussian matching
317 probabilities are done by the equations:

$$318 \quad \mu_{k-1}^{ij} = \frac{1}{t_j} O_{ij} \mu_{k-1}^i \quad (15)$$

319 The normalization factor is given as per the following:

$$320 \quad \bar{t}_j = \sum_{i=1}^r O_{ij} \mu_{k-1}^{ij} \quad (16)$$

321 The matching possibility model μ_k^{ij} is updated under model
322 likelihood and model transition possibility controlled via the
323 IFL as per the following:

$$324 \quad \mu_k = \frac{1}{t} A_k^j \bar{t}_j \quad (17)$$

325 wherever

$$326 \quad t = \sum_{j=1}^r \bar{t}_j A_k^j \quad (18)$$

327 And A_k^j is a likelihood function as per the following:

$$328 \quad A_k^j = \frac{1}{\sqrt{2\pi} |P_{x_k x_k}^j|} \exp \left[-\frac{1}{2} (Z_k - \bar{Z}_k)^T (P_{x_k x_k}^j)^{-1} \right] \quad (19)$$

$$329 \quad \gamma_k = (1 - \mu_k)^d, d \geq 1 \quad (20)$$

330 wherein s and c are the standard deflections and the center
331 of the Gaussian basis function, d is a parameter that must be
332 designed. If $d = 0, \mu_A + \gamma_A = 1$ and the hesitation degree π_A

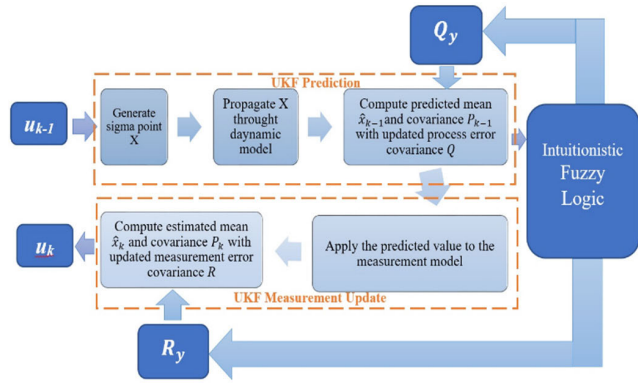


FIGURE 1. Hybrid filter CLAM framework.

also is zero. The NMD and MD of the i^{th} rule are represented as per the following:

$$\bar{\mu}_j = \mu_{1j}\mu_{2j} \dots \mu_{nj} = \prod_{i=1}^n \mu_{ij} \quad (21)$$

$$\bar{\gamma}_j = \gamma_{1j}\gamma_{2j} \dots \gamma_{nj} = \prod_{i=1}^n \gamma_{ij} \quad (22)$$

It normalized the NMD and MD of the fuzzy and computed the hesitation margin index.

$$\bar{\varphi}_j = \frac{\bar{\mu}_j}{\sum_{j=1}^m \bar{\mu}_j} \quad (23)$$

$$\bar{\theta}_j = \frac{\bar{\gamma}_j}{\sum_{j=1}^m \bar{\gamma}_j} \quad (24)$$

$$\pi_j = 1 - \bar{\varphi}_j - \bar{\theta}_j \quad (25)$$

The output of the intuitionistic fuzzy with n rules can be computed as per the following:

$$y = \sum_{j=1}^m \left((1 - \pi_j) s_j \bar{\varphi}_j + \pi_j \bar{s}_j \bar{\theta}_j \right) = \sum_{j=1}^m y_j \quad (26)$$

The polynomial parameter s_i can be solved via least square regression techniques. If $O_{ij} = Q$ then, will construct Q_y or $O_{ij} = R$ then construct R_y .

Finally, the Pseudocode of the IFL phase for the selection of the best SPs is given in Algorithm 1.

B. THE HYBRID FILTER CLAM PREDICTION STAGE

The Hybrid filter is explained using the poses of a robot and features, including the position of landmarks. For the CLAM, the main robot motion requirements are to be offered. The Hybrid filter CLAM framework has a few privileges in management robot navigation with nonlinear movements owing to the inference feature of the IFL, which also needs a fewer quantity of comparisons than the UFS and shows much better efficiency from the robustness, perspective assessment exactitude, and reliability than the UFS. The Hybrid filter CLAM framework, as shown in Fig. 1.

The following state equation shows a configuration of the robot, $X^a = (x^{\theta} Q_y R_y)^T$ as per the following:

$$X_k^a = \begin{bmatrix} x_k \\ y_k \\ \theta_k \\ Q_{y,k} \\ R_{y,k} \end{bmatrix} = \begin{bmatrix} x_{k-1} + v_k \Delta t \cos(\theta_k) \\ y_{k-1} + v_k \Delta t \sin(\theta_k) \\ \theta_{k-1} + v_k \Delta t \sin(\frac{\Delta \theta}{L}) \\ Q_{y,k-1} \\ R_{y,k} - 1 \end{bmatrix} \quad (27)$$

$$u_k = v_k + N(0, M_k) \quad (28)$$

The wheels velocity is v_k , Δt is the sampling period and L is the distance between the robot's wheels. Eventually, M_k demonstrates the MNCM period. The vector Y_k is a combination of X^a and the position of the robot as per the following:

$$Y_k^a = \begin{bmatrix} X_k^a \\ m \end{bmatrix} = (x_k y_k \theta_k Q_{y,k} R_{y,k}, m_{k,x}^i m_{k,y}^i s_k^i 00)^T \quad (29)$$

The probability of X^a as per the following:

$$X_k^a = f(X_{k-1}^a, u_{k-1}) + N(0, Q_{y,k}) \quad (30)$$

wherein f demonstrates the nonlinear functions, $Q_{y,k}$ is the procedure noise, and u_k is an input of control. The f it is partial insulate is utilized with X_k^a for the Taylor extension of function, as per the following:

$$\hat{f}(X_{k-1}^a, u_k) = \frac{\partial f(X_{k-1}^a, u_k)}{\partial X_k^a} \quad (31)$$

f is approximated at u_k and u_{k-1} . The linear extraction is arrived at using the gradient of f at u_k and u_{k-1} as per the following:

$$f(X_{k-1}^a, u_k) = f(u_{k-1}, u_k) + \hat{f}(u_{k-1}, u_k)(X_k^a, u_{k-1}) \quad (32)$$

With the substitution quantities acquired from Eqs. (1-5), the previous covariance and mean as per the following:

$$\hat{x}_k = \sum_{i=0}^{2n} w_i X_{i,k}^a \quad (33)$$

As explained in Eq.(34), the observation model Z_k involves the observation noise $R_{y,k}$, and nonlinear measurement function h, m involved vector of landmark,s pose.

$$Z_k = h(Y_k^a) + N(0, R_{y,k}) = \begin{bmatrix} \sqrt{(m_{k,x}^i - x_k)^2 + (m_{k,y}^i - y_k)^2} \\ \tan^{-1} \left(\frac{m_{k,y}^i - y_k}{m_{k,x}^i - x_k} \right) - \theta_k \end{bmatrix} + N(0, R_{y,k}) \quad (34)$$

$$m^i = (m_x^i m_y^i)^T \quad (35)$$

$$\bar{Z}_k = \sum_{i=0}^{2n} w_i Z_k \quad (36)$$

Algorithm 1: Pseudo-Code for the IFL Phase for Choosing the Best Weight for SP

- 1: **for** $i=1$ to r
- 2: **for** $i=1$ to r
- 3: computing of state probabilities model O_{ij} (14)
- 4: computing the matching probabilities μ_{k-1}^{ij} (15)
- 5: computing the normalization factor \bar{t}_j (16)
- 6: update matching probabilities model μ_k^{ij} (17),(18),(19)
- 7: computing the likelihood function A_k^j (7),(8),(9)
- 8: computing MD and NMD $\bar{\mu}_j, \bar{\nu}_j$ (21),(22)
- 9: computing normalization of membership and non-membership $\bar{\theta}_j, \bar{\varphi}_j$ (23),(24)
- 10: computing the hesitation degree π_j (25)
- 11: **end for**
- 12: **end for**
- 13: computing the output of the IFL system y (26)

391 **C. THE HYBRID FILTER CLAM MEASUREMENT UPDATE**
392 **STAGE**

393 To attain the Kalman gain K_k , we should compute $P_{x_k x_k}$ and
394 $P_{x_k y_k}$. To get the amounts $P_{x_k x_k}$ and $P_{x_k y_k}$, we require to
395 calculate $\hat{x}_k, Z_k, \bar{Z}_k$ that derived from equations 27, 33, 34,
396 36, by the substitution of these quantities, we will have as per
397 the following:

$$398 \quad P_{x_k x_k} = \sum_{i=0}^{2n} w_i [Z_{i,k} - \bar{Z}_k][Z_{i,k} - \bar{Z}_k]^T + R_{y,k} \quad (37)$$

$$399 \quad P_{x_k y_k} = \sum_{i=0}^{2n} w_i [X_{i,k}^a - \hat{x}_k][Z_{i,k} - \bar{Z}_k]^T \quad (38)$$

$$400 \quad K_k = P_{x_k y_k} P_{x_k x_k}^{-1} \quad (39)$$

401 In the again sampling stage, some SPs with moderately huge
402 jumbles with their objective, called bad SPs, are dismissed.
403 Other SPs with moderately huge jumbles with their objective,
404 is called good SPs. Nevertheless, the UFS has been patronizing
405 the SP reduction issue and the filter convergence issue that
406 are via the mistake weights, the rejection, and replication
407 during the again sampling phase, but the Hybrid filter CLAM
408 does not have these issues. The IFL system includes inference
409 using measurement quantities and input quantities. The next
410 stage to attain the previous covariance and mean is to reform
411 the results. The procedure mentioned in the top five stages
412 iterates at the end of the navigation.

$$413 \quad \hat{x}_k = \hat{x}_k + K_k(Z_k - \bar{Z}_k) \quad (40)$$

$$414 \quad P_k = P_k - K_k P_{x_k x_k} K_k^T \quad (41)$$

415 Finally, the Hybrid filter CLAM pseudocode is given in Algo-
416 rithm 2.

417 **IV. SIMULATION AND EXPERIMENTAL ANALYSIS**

418 The Python code, to demonstrate the efficiency of the
419 Hybrid filter CLAM expanded by Atsushi, was modified [25]. In this paper, two navigation types of a robot
420 are surveyed: Floor navigation, and Victoria Park naviga-
421 tion. peculiarities of the navigation maps are explained in
422 Table 1.
423

TABLE 1. Main specifications for navigation.

| Item | Floor | Victoria Park |
|----------|-------|---------------|
| Feature | 17 | 73 |
| Waypoint | 18 | 79 |
| Area[m] | 16*17 | 250*300 |

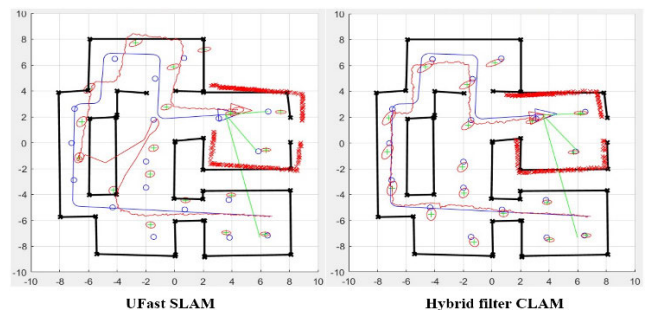


FIGURE 2. Navigation result in the floor map.

A. NAVIGATION RESULTS IN THE FLOOR MAP

424 In this case of the floor navigation, navigation according to the Hybrid filter CLAM and UFS. The results are based
425 on competition of the UFS and Hybrid filter CLAM. The navigation pursuant to both methods is illustrated in Fig. 2.
426 The efficiency of the Hybrid filter CLAM is compared to UFS where its MNMCM is maintained stationary. The proposed
427 method wrongly adapts MNMCM and CMPN matrix in UKF using IFL and decides to a minimum the conformity between
428 the actual and theoretical quantities of the innovation procedure in UKF. The robot specifies a direction pursuant to
429 the data from the locations of landmarks identified for the navigation, but due to unpredictable changes in incoming
430 data, it does not right away turn in the edges. The paths a robot must cover are shown with the blue line, the robot path
431 is shown with the red line and the laser rays are shown with a green line. The location of the landmarks is shown with
432 the plus points (+).
433
434
435
436
437
438
439
440
441

Algorithm 2: Pseudocode of the Hybrid Filter CLA

- 1: Initialization parameters
- 2: for $k = 1$ to M
- 3: % state estimation of Robot
- 4: Extract the robot position x_k using SPs collection X_{k-1} (2),(6)
- 5: Predict mean \hat{x}_k (4) and covariance P_k (5) of robot associate observation data
- 6: Attain the robot predicted covariance
- 7: for $k =$ known feature
- 8: Update mean \hat{x}_k (12) and covariance P_k (13) of the robot
- 9: Update SPs (30)
- 10: Compute importance weight w_i (33)
- 11: end for
- 12: % position estimation of environmental features
- 13: if $k =$ new feature
- 14: Initialize new feature mean \hat{x}_k and covariance P_k
- 15: else
- 16: Update mean (39) and covariance (40) of features
- 17: end if
- 18: end for

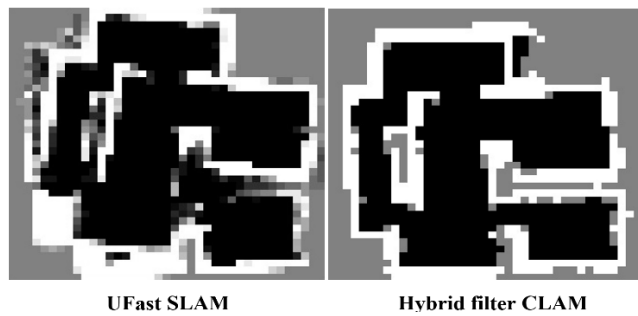


FIGURE 3. Mapping result in the floor map.

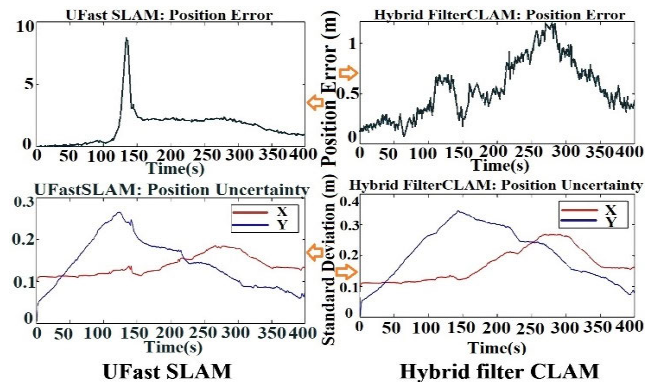


FIGURE 4. Errors and incertitude of position in the floor map.

In Fig. 3, are shown generated maps via the received data. Because the proposed method detects the position of landmarks more carefully, this can construct required maps of the mapping stage with the GICP method, more carefully. We were able to decline the iterative matching procedure to estimate the robot pose and construct a 2D map. The proposed method was able to quickly obtain the robot pose and make a map. Also, the proposed method is more precise.

In Fig. 4, the errors and incertitude of position for the UFS and Hybrid filter CLAM, respectively. By comparing the ultimate approximation of the position and the real position deflection, the standard deflection curve of the position deflection and the state amount of x, y are shown in Fig. 4.

Generally, the position deflection attained via the Hybrid filter CLAM is fewer than that of the UFS deflection. These deflections may demonstrate that there is no good deflection control to calculate for the robot's rotation. Generally, ameliorated position deflection of the Hybrid filter CLAM is well preserved at around 0.2 m, so the IFL has good efficacy on positioning exactitude. Amid the total procedure of robot navigation, the localization error always has a small range,

and the robustness of the Hybrid filter CLAM is effectually ameliorated.

In Fig. 5, simultaneously errors of the angular and position in scan and odometry state for the UFS and Hybrid filter CLAM, respectively. The angular deflection and position deflection of the motion model is computed via an odometer and scan matching is shown in Fig. 5.

From the Hybrid filter CLAM, it is made clear the angle and position deflection will be confirmed, amid which the position and angle deflection of the odometer motion model gotten to be litter. The relevant weights are adjusted to ensure the exactitude of the position assessment and prediction stage.

Table 2 provides the running time and the RMSE of the mobile robot position of the Hybrid filter CLAM compared to the UFS. The results illustrate that Hybrid filter CLAM ameliorates the positioning exactitude of a robot compared to the UFS in the floor Map. Moreover, the Hybrid filter CLAM utilized a shorter running time of 7.1 %. Therefore, the Hybrid filter CLAM has better computational efficiency exactitude

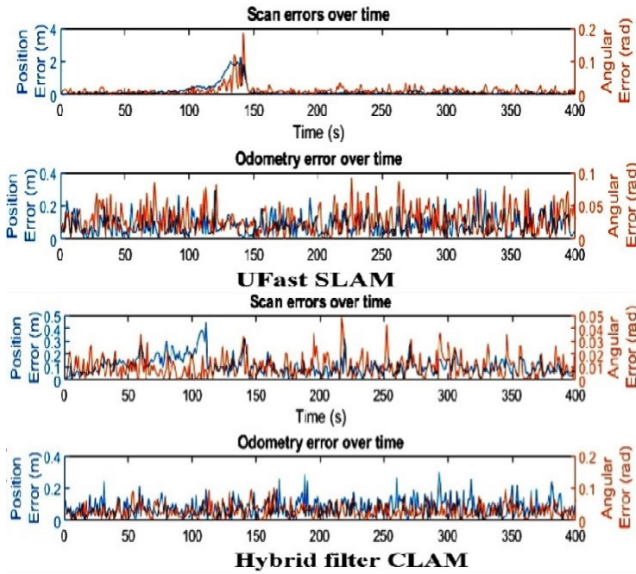


FIGURE 5. Simultaneously errors of the angular and position in scan and odometry state in the floor map.

TABLE 2. RMSE of running time and vehicle position of methods in the floor map.

| Methods | RMSE(m) | Cost time(s) |
|--------------------|---------|--------------|
| UFS | 2.845 | 35.2 |
| Hybrid filter CLAM | 0.968 | 32.7 |

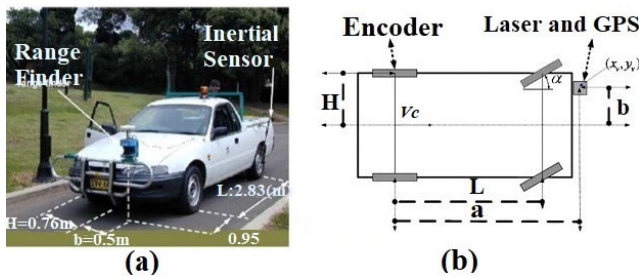


FIGURE 6. (a) The mobile vehicle was utilized for data collection. (b) The motion model of mobile vehicle [27].

482 than the UFS. This can be since the Hybrid filter CLAM
 483 adaptively adjusted the MNMCM and CMPN. These matrices
 484 merge to the actual MNMCM and CMPN while MNMCM and
 485 CMPN in UFS are constant over time.

486 **B. EXPERIMENTAL RESULT OF NAVIGATION WITH**
 487 **“VICTORIA PARK DATASET”**

488 The experiment is carried out in the Victoria Park dataset
 489 until validation of the efficiency of the proposed method
 490 is illustrated for solving the CLAM problem. The Victoria
 491 Park dataset was gathered via the Australian Centre for Field
 492 Robotics in Victoria Park. The vehicle provided with different
 493 sensors is shown in Figure 7a. The environment is the trajec-
 494 tory is long (4.5 km), large (250 × 300), and there are many

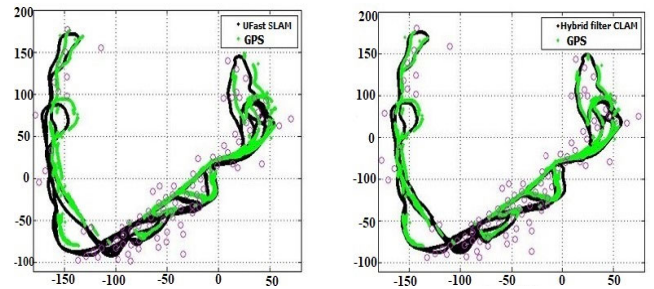


FIGURE 7. Experimental results in the Victoria Park map.

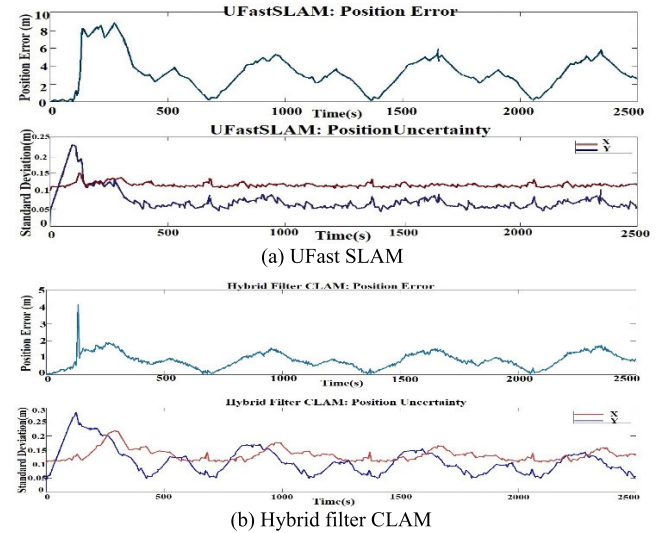


FIGURE 8. (a) and (b) errors and incertitude of position in the Victoria Park map.

495 loops (14 loops). The observations have much spurious detec-
 496 tion of trees. Figure 8 shows the map and trajectory created
 497 via the Hybrid filter CLAM and FastSLAM. In both methods,
 498 the free parameters, such as covariance matrices of noises and
 499 error bounds, are chosen via the error and experiment method.
 500 A GPS was utilized to supply ground truth data, steering angle
 501 and vehicle velocity were gathered with an inertial sensor.
 502 A laser range finder was utilized to the bearing landmarks and
 503 measure the range with the vehicle. Therefore, those observa-
 504 tions with high gravity data are exploited from laser
 505 data as eventual landmarks, and the nearest neighbor method
 506 is utilized for the data association step [26]. The different
 507 sensors of the vehicle are shown in Fig 6a [26]. Fig 6 shows
 508 the map and path made using the Hybrid filter CLAM and
 509 UFS. In both methods, covariance matrices of noises and
 510 error bounds are chosen by the experiment and error method.
 511

512 The vehicle structure is shown in Fig. 6a. The motion
 513 model is illustrated as per the following:

$$x_v = v \cos(\theta), \quad y_v = v \sin(\theta) \text{ and } \dot{\theta}_v = v |L \tan(\alpha) \quad (44)$$

514 The motion model of the mobile vehicle shown in Fig. 6b
 515 and Eq. (44) demonstrates the pose of the back axle,
 516

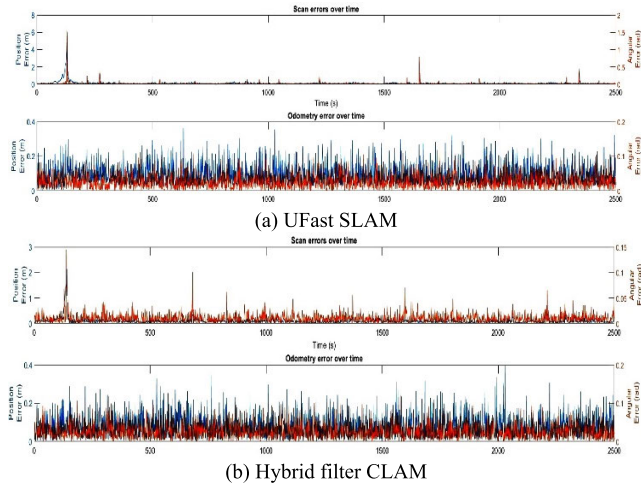


FIGURE 9. Simultaneously angular and position of the error in scan and odometry state in the Victoria Park maps.

but a Global Positioning System (GPS) and laser range finder are installed at the front of the vehicle. Therefore, to simplify the update procedure, the motion model must be reformed to illustrate the GPS pose and laser sensor. The discrete motion model is explained as per the following: [28]. (42) and (43), as shown at the bottom of the page, wherever the sampling time is t and v is the velocity is v , but v_e get from the sensor demonstrates the velocity of the left rear wheel. The navigation pursuant to the UFS and Hybrid filter CLAM is illustrated in Fig. 7, wherever more deflections are shown on corners with bigger angles during the navigation procedure.

The vehicle determines a direction for the navigation pursuant to the data from the landmarks identified positions. The green line is shown the mobile robot paths with GPS data should be covered and the robot path is shown with a black line, pursuant to data explained via the Hybrid filter CLAM. The pink circle (o) describes the location of the landmark that is known and stationary in the area.

The efficiency of the Hybrid filter CLAM is better than that of the UFS. Also, the efficiency of the UFS and Hybrid filter CLAM depends on increasing the number of loops and the number of hypothetical Jacobians.

Also, when the Hybrid filter CLAM and UFS are utilized to solve a variety of issues with higher dimension variable complexity more nonlinear systems may be incremented.

TABLE 3. RMSE of running time and vehicle position of methods in the Victoria Park map.

| Methods | RMSE(m) | Cost time(s) |
|--------------------|---------|--------------|
| UFS | 5.96 | 1434.9 |
| Hybrid filter CLAM | 2.47 | 1563.2 |

In Fig. 8, position errors and position incertitude of the Hybrid filter CLAM and UFS, respectively.

By comparing the ultimate approximation of the position and the real position deflection, the standard deflection curve of the position deflection and the state amount of x and y are shown in Fig. 8.

Generally, the position deflection attained via the Hybrid filter CLAM is fewer than that of the UFS deflection. These deflections may demonstrate that there is no good deflection control to calculate for the robot's rotation. Generally, ameliorated position deflection of Hybrid filter CLAM is well maintained at around 0.15 m, so the IFL has good efficacy on positioning exactitude. Amid the total procedure of robot navigation, the localization error always has a small range, and the robustness of the Hybrid filter CLAM is effectually ameliorated.

In Fig. 9, simultaneously errors of the angular and position in scan and odometry state for the UFS and Hybrid filter CLAM, respectively. The angular deflection and position deflection of the motion model is computed via an odometer and scan matching is shown in Fig. 9.

From the Hybrid filter CLAM, it is made clear the angle and position deflection will be confirmed, amid which the position and angle deflection of the odometer motion model gotten to be litter. The relevant weights are adjusted to ensure the exactitude of the position assessment and prediction stage.

Table 3 provides the running time and the RMSE of the mobile robot position of the Hybrid filter CLAM compared to the UFS. The results illustrate that Hybrid filter CLAM ameliorates the positioning exactitude of a robot compared to the UFS in the Victoria park Map. Moreover, the Hybrid filter CLAM utilized a shorter running time of 8.9%. Therefore, the Hybrid filter CLAM has better computational efficiency exactitude than the UFS. This can be since the Hybrid filter CLAM adaptively adjusted the MNCM and CMPN. These matrices merge to the actual MNCM and CMPN while MNCM and CMPN in UFS are constant over time.

$$\begin{bmatrix} x_{k,v} \\ y_{k,v} \\ \theta_{k,v} \end{bmatrix} = \begin{bmatrix} x_{k-1,v} + \Delta t(v_{k-1} \cos(\theta_{k-1,v}) - \frac{v_{k-1}}{L} \tan(\alpha_{k-1})(a \sin(\theta_{k-1,v}) + b \cos(\theta_{k-1,v}))) \\ y_{k-1,v} + \Delta t(v_{k-1} \sin(\theta_{k-1,v}) + \frac{v_{k-1}}{L} \tan(\alpha_{k-1})(a \cos(\theta_{k-1,v}) + b \sin(\theta_{k-1,v}))) \\ \theta_{k-1,v} + \Delta t \frac{v_{k-1}}{L} \tan(\alpha_{k-1}) \end{bmatrix} + W_{k-1} \quad (42)$$

$$v_{k-1} = \frac{v_{k-1,e}}{1 - \frac{H}{L} \tan(\alpha_{k-1})} \quad (43)$$

V. CONCLUSION

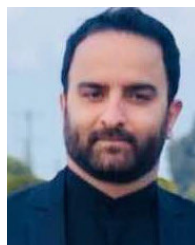
This paper, proposes a new method with the name of Hybrid filter CLAM for the navigation procedure of a robot. It is concluded with the correction of the formula utilized to compute the linear approximation process and the observation function Jacobian matrix. The incorrect previous information around the CMPN and MNMCM may many declines the efficiency of UFS. An additional stage for adjusting the CMPN and MNMCM is proposed in the proposed method. To decline the efficacy of the cumulative. Based on the results, the UFS has more errors than the Hybrid filter CLAM and can ameliorate the exactitude of assessment and maintain diversity. It does not utilize the linear approximations and the production of the Jacobian matrices in the UKF framework is a significant benefit and updates the mean and covariance of the attribute state via utilizing the unscented filter. In the localization procedure, the Hybrid filter CLAM is developed in the prediction stage of the robot state, and the UKF offers improved proposal distribution without computing the Jacobian matrices. The IFL is engaged in dynamically regulating the MNMCM and CMPN. When a designer does not have to equate information to extend the complete filter models or when the filter parameters are sedately changing with time, the IFL can be engaged to ameliorate the UFS efficiency. The proposed method It does not use the production of the Jacobian matrices and linear approximations to the nonlinear functions in the UFast-SLAM is the major advantage of this method and updates the covariance and mean of the feature state via IFLS in the feature estimation. The proposed method has the additional benefit of decreasing the quantity of SPs when maintaining the assessment exactitude. In addition, the results admit that the Hybrid filter CLAM is better for navigation procedure results, and also the consistency is higher than that of the UFS. However, computational complexity is incremented using more hypothetical Jacobians. Also, exploiting the proposed method to a more nonlinear system may increment the complexity with higher dimension variables. Therefore, it is significant to make a tradeoff between assessment exactitude and computational complexity. In addition, decreasing the Kalman filters family dependent on the characteristic of a system such as nonlinearity and dimension variables can be a great research subject in the future and also use another meta heuristic method for improvement of the sampling process.

Funding Statement: The authors received no specific funding for this study. Conflicts of Interest: The authors declare that they have no conflicts of interest to report regarding the present study.

REFERENCES

- [1] J.-H. Kim and G. I. Kim, "Extended Kalman filter based mobile robot localization in indoor fire environments," *Int. J. Mech. Eng. Robot. Res.*, vol. 5, no. 1, pp. 62–66, 2016.
- [2] P. Zhu, G. Wei, and J. Li, "On hybrid consensus-based extended Kalman filtering with random link failures over sensor networks," *Kybernetika*, vol. 56, no. 1, pp. 189–212, Apr. 2020, doi: [10.14736/kyb-2020-1-0189](https://doi.org/10.14736/kyb-2020-1-0189).
- [3] D. Lee, G. Vukovich, and R. Lee, "Robust unscented Kalman filter for nanosat attitude estimation," *Int. J. Control, Autom. Syst.*, vol. 15, no. 5, pp. 2161–2173, Oct. 2017.
- [4] C. Kim, R. Sakthivel, and W. K. Chung, "Unscented FastSLAM: A robust and efficient solution to the SLAM problem," *IEEE Trans. Robot.*, vol. 24, no. 4, pp. 808–820, Aug. 2008.
- [5] Y. Zhao, S.-S. Gao, J. Zhang, and Q.-N. Sun, "Robust predictive augmented unscented Kalman filter," *Int. J. Control, Autom. Syst.*, vol. 12, no. 5, pp. 996–1004, Oct. 2014.
- [6] S. Zeghlache, D. Saigaa, and K. Kara, "Fault tolerant control based on neural network interval type-2 fuzzy sliding mode controller for octorotor UAV," *Frontiers Comput. Sci.*, vol. 10, pp. 657–672, Aug. 2016, doi: [10.1007/s11704-015-4448-8](https://doi.org/10.1007/s11704-015-4448-8).
- [7] P. A. D. Harischandra and A. M. H. S. Abeykoon, "Intelligent bimanual rehabilitation robot with fuzzy logic based adaptive assistance," *Int. J. Intell. Robot. Appl.*, vol. 3, no. 1, pp. 59–70, Mar. 2019.
- [8] M. Y. Chen, "The SLAM algorithm for multiple robots based on parameter estimation," *Intel. Auto. Soft Comput.*, vol. 24, no. 3, pp. 593–602, 2018.
- [9] A. Al-Hourani and B. Ristic, "MapperBot/iSCAN: Open-source integrated robotic platform and algorithm for 2D mapping," *Int. J. Intell. Robot. Appl.*, vol. 4, no. 1, pp. 44–56, Mar. 2020.
- [10] R. Havangi, "A mutated FastSLAM using soft computing," *Ind. Robot Int. J.*, vol. 44, no. 4, pp. 416–427, Jun. 2017, doi: [10.1108/IR-11-2016-0277](https://doi.org/10.1108/IR-11-2016-0277).
- [11] K. Karnavel, G. Shanmugasundaram, S. S. Salunkhe, V. K. Sundari, M. Shunmugathammal, and B. K. Saraswat, "Actuator fluid control using fuzzy feedback for soft robotics activities," *Intell. Autom. Soft Comput.*, vol. 32, no. 3, pp. 1855–1865, 2022, doi: [10.32604/iasc.2022.023524](https://doi.org/10.32604/iasc.2022.023524).
- [12] N. Vafamand, M. M. Arefi, and A. Khayatian, "Nonlinear system identification based on Takagi-Sugeno fuzzy modeling and unscented Kalman filter," *ISA Trans.*, vol. 74, pp. 134–143, Mar. 2018.
- [13] L. Qiu and H. Ren, "Endoscope navigation with SLAM-based registration to computed tomography for transoral surgery," *Int. J. Intel. Rob. App.*, vol. 4, pp. 252–263, Apr. 2020, doi: [10.1007/s41315-020-00127-2](https://doi.org/10.1007/s41315-020-00127-2).
- [14] K. R. Hamid, A. Talukder, and A. K. M. E. Islam, "Implementation of fuzzy aided Kalman filter for tracking a moving object in two-dimensional space," *Int. J. Fuzzy Log. Intell. Syst.*, vol. 18, no. 2, pp. 85–96, Jun. 2018, doi: [10.5391/IJFIS.2018.18.2.85](https://doi.org/10.5391/IJFIS.2018.18.2.85).
- [15] A.-W. A. Saif, M. Atau-Rahman, S. Elferik, M. F. Mysorewala, M. Al-Dhaifallah, and F. Yacef, "Multi-model fuzzy formation control of UAV quadrotors," *Intell. Autom. Soft Comput.*, vol. 27, no. 3, pp. 817–834, 2021.
- [16] J. Dai, X. Li, K. Wang, and Y. Liang, "A novel STSOSLAM algorithm based on strong tracking second order central difference Kalman filter," *Robot. Auto. Syst.*, vol. 116, pp. 114–125, Jun. 2019, doi: [10.1016/j.robot.2019.03.006](https://doi.org/10.1016/j.robot.2019.03.006).
- [17] M. Lin, C. Yang, and D. Li, "An improved transformed unscented Fast-SLAM with adaptive genetic resampling," *IEEE Trans. Ind. Electron.*, vol. 66, no. 5, pp. 3583–3594, May 2019, doi: [10.1109/TIE.2018.2854557](https://doi.org/10.1109/TIE.2018.2854557).
- [18] M. G. H. Nampoothiri, P. S. G. Anand, and R. Antony, "Real time terrain identification of autonomous robots using machine learning," *Int. J. Intell. Robot. Appl.*, vol. 4, no. 3, pp. 265–277, Sep. 2020.
- [19] A. Bakdi, A. Hentout, and H. Boutami, "Optimal path planning and execution for mobile robots using genetic algorithm and adaptive fuzzy-logic control," *Robot. Auto. Syst.*, vol. 89, no. 1, pp. 95–109, 2017, doi: [10.1016/j.robot.2016.12.008](https://doi.org/10.1016/j.robot.2016.12.008).
- [20] S. J. Julier and J. K. Uhlmann, "Unscented filtering and nonlinear estimation," *Proc. IEEE*, vol. 92, no. 3, pp. 401–422, Mar. 2004.
- [21] M. Turan, Y. Almalioglu, H. Araujo, E. Konukoglu, and M. Sitti, "A non-rigid map fusion-based direct SLAM method for endoscopic capsule robots," *J. Intell. Robot. Appl.*, vol. 1, no. 4, pp. 399–409, 2017, doi: [10.1007/s41315-017-0036-4](https://doi.org/10.1007/s41315-017-0036-4).
- [22] G. Klanar, L. Teslic, and I. Skrjanc, "Mobile robot pose estimation and environment mapping using an extended Kalman filter," *Int. J. Sys. Sci.*, vol. 26, pp. 1–16, Dec. 2013, doi: [10.1080/00207721.2013.775379](https://doi.org/10.1080/00207721.2013.775379).
- [23] X. Peng, B. Zhang, and L. Rong, "A robust unscented Kalman filter and its application in estimating dynamic positioning ship motion states," *J. Mar. Sci. Technol.*, vol. 24, no. 4, pp. 1265–1279, Dec. 2019, doi: [10.1007/s00773-019-00624-5](https://doi.org/10.1007/s00773-019-00624-5).
- [24] A. Rodriguez-Angeles and L. F. Vazquez-Chavez, "Bio-inspired decentralized autonomous robot mobile navigation control for multi agent systems," *Kybernetika*, vol. 54, no. 1, pp. 135–154, 2018.
- [25] (2018). *Atsushi Sakai*. [Online]. Available: <https://atsushisakai.github.io>
- [26] E. Nebot. (2008). *Victoria Park Dataset*. [Online]. Available: <http://www-personal.acfr.usyd.edu.au/nebot/dataset.htm>

710 [27] W. Zhou, C. Zhao, and J. Guo, "The study of improving Kalman filters
 711 family for nonlinear SLAM," *J. Intell. Robot. Syst.*, vol. 56, no. 5,
 712 pp. 543–564, Dec. 2009, doi: [10.1007/s10846-009-9327-9](https://doi.org/10.1007/s10846-009-9327-9).
 713 [28] J. Guivant, E. Nebot, and S. Baiker, "Autonomous navigation and map
 714 building using laser range sensors in outdoor applications," *J. Robot. Syst.*,
 715 vol. 17, no. 10, pp. 565–583, Oct. 2000.



JAVAD MASOUDI received the B.S., M.S., and
 Ph.D. degrees in computer engineering from
 Islamic Azad University, Sari, Iran, in 2007,
 2014, and 2020, respectively. His research inter-
 ests include cloud computing and task scheduling.

737
738
739
740
741



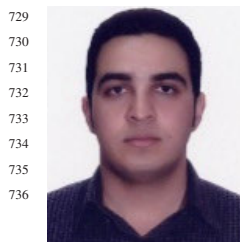
YONG FANG was born in Jiangxi, China, in 1984.
 He received the B.S. degree in electronic and infor-
 mation engineering specialty from the Guilin Uni-
 versity of Electronic Technology, China, in 2003,
 the M.S. degree in pattern recognition and intelli-
 gent system from Xidian University, Xi'an, China,
 in 2011, and the Ph.D. degree in information
 from the Université de technologie de Belfort-
 Montbéliard, Belfort, France, in 2015. Since 2016,
 he has been a Lecturer with the Department of
 Traffic and Transportation, Chongqing Jiaotong University, Chongqing.
 He is the author of more than five articles. His research interests include
 machine learning, image processing, and robotic.

716
717
718
719
720
721
722
723
724
725
726
727
728



BEHNAM BARZEGAR received the B.S. degree
 in computer engineering from Islamic Azad Uni-
 versity, Sari, Iran, in 2006, the M.S. degree in com-
 puter engineering from Islamic Azad University,
 Najafabad, Iran, in 2009, and the Ph.D. degree in
 computer engineering from Islamic Azad Univer-
 sity at Sari, in 2018. He is currently an Associate
 Professor with the Department of Computer Engi-
 neering, Islamic Azad University at Babol, Babol,
 Iran. His research interests include green cloud
 computing, task scheduling, and formal methods (petri net).

742
743
744
745
746
747
748
749
750
751
752



AMIR PANAH received the B.S. degree from
 the Iran University of Science and Technology,
 Iran, in 2008, the M.S. degree from Islamic Azad
 University, Qazvin, Iran, in 2011, and the Ph.D.
 degree from Islamic Azad University, Babol, Iran,
 in 2021. His research interests include SLAM,
 mobile robot, rescue robot, and artificial intelli-
 gence.

729
730
731
732
733
734
735
736



SAEED FATEHI received the M.S. degree in com-
 puter engineering and software engineering from
 Islamic Azad University, Iran. He is currently pur-
 suing the Ph.D. degree in software engineering
 with Islamic Azad University, Babol, Iran. His
 current research interests include software quality
 and cloud computing.

753
754
755
756
757
758
759
760

